

Processing History in Extrusion Dies and Its Influence on the State of the Polymer Extrudate at the Die Exit*

HORST HENNING WINTER

*Department of Chemical Engineering
University of Massachusetts
Amherst, Massachusetts 01003*

and

ERNST FISCHER

*Institut für Kunststofftechnologie
Universität Stuttgart
7 Stuttgart-1, West Germany*

(accepted Jan 8, 1980)

A method is proposed to describe the processing history in extrusion dies and its influence on the state of the polymer after processing. The approach differs from conventional processing analysis, which uses the shear viscosity function to calculate pressure drop vs flow rate relations. The approach also differs from heuristic analysis which tries to find empirical correlations between rheological observations and processing behavior. The method is applied to the flow in annular extrusion dies. An integral constitutive equation is chosen to calculate the flow and to describe the flow history at the die exit as memorized. In the analysis, the kinematics are locally approximated by isothermal steady shear flow. The velocity and the velocity gradient are used to determine the Finger strain tensor, the path lines, and the residence times of the deforming material elements. Measures of the state of the polymer at the die exit are chosen to be the stress ratio $N_1/2\tau_{12}$ and the free recovery. The free recovery calculations presume that the extrudate is chopped into small volumes of homogeneous flow history. The results of the calculations show the polymer very sensitively reacts to small changes of the die geometry. Important applications of this analysis are film blowing and blow molding, where the extensional behavior during the blowing process outside the die depends greatly on the preceding shaping process inside the die.

INTRODUCTION

Although an enormous amount of literature has been devoted to the study of polymer processing (see for instance recent text books (1-3)) there still exists a need for a better qualitative and quantitative understanding of the relation between processing history and the end use properties of polymeric products. This understanding can be gained by studying the processing history of individual material elements in the processing equipment, e.g., in an extruder or an injection molding machine. Along its path through the machine, the material elements are subjected to large strains and to changing temperatures. The final polymeric product then consists of material elements with a variety of individual processing histories. The polymer, therefore, might be very inhomogeneous with respect to its local mechanical or optical properties. The integral over this distribution of properties determines the overall performance of the polymeric product.

* presented at the VIII Int Congr. Rheology, Naples 1980

The goal of the following study is a description of the state of a polymer when extruded from an annular extrusion die. The annular geometry has been chosen because it is common for various extrusion dies (pipe extrusion, film blowing, blow molding). It is still simple enough to be tractable for a detailed flow analysis and for the development of new analytical methods. The annular geometry makes it possible to generate flow histories with shear and biaxial extension superimposed (by changing the radius and the gap width along the annulus). The study is concerned with polymers in the molten state, only.

RHEOLOGICAL CONSTITUTIVE EQUATIONS

During the last 30 years a large number of possible constitutive equations have been proposed and tested experimentally; see, for instance, (4). At least one group of these equations seems to be sufficiently accurate in describing the rheological behavior of molten polymers,

and it is still fairly simple to use in flow calculations. This is the rubber-like liquid equation of Lodge (5) as modified by Kaye (6) and Bernstein, Kearsley and Zapas (7):

$$\underline{\sigma}(t) = -p(t)\underline{1} + \int_{-\infty}^t m(t', t) \underline{C}^{-1}(t', t) dt' \quad (1)$$

where $\underline{\sigma}(t)$ is the stress at time t , p the isotropic pressure contribution, $\underline{1}$ the unit tensor, $m(t', t)$ the memory functional, and $\underline{C}^{-1}(t', t)$ the relative Finger strain tensor between time t' and t .

The material behavior is contained in the memory functional $m(t', t)$ which not only depends on the time difference $t - t'$ (as the rubber-like liquid (5) does), but also on the time dependent invariants of the strain tensor \underline{C}^{-1} . Various types of memory functionals have been suggested in the literature. A very successful form which has been proposed by several authors (8-14) uses a product of two separate functions (or functionals) for the strain dependence and for the time dependence of the memory functional

$$m(t', t) = h(t', t) \dot{m}(t - t') \quad (2)$$

The strain functional h depends on the three invariants $I(t', t)$, $II(t', t)$, and $III(t', t)$ of the Finger strain tensor. The influence of the third invariant will be neglected by assuming constant density. The memory function $\dot{m}(t - t')$ of linear viscoelasticity (see (21)) depends only on the time difference $t - t'$. It may be described by a discrete relaxation spectrum

$$\dot{m}(t - t') = \sum_{i=1}^N \frac{G_i}{\lambda_i} \exp\left(-\frac{t - t'}{\lambda_i}\right) \quad (3)$$

where G_i are the relaxation moduli and $\lambda_i(T)$ the temperature dependent relaxation times.

The constitutive equation, Eq 1 with Eqs 2 and 3, has been tested extensively by Wagner and Laun (15-19) and was found to describe all phenomena in shear and uniaxial extension of a low density polymer sample (called "melt I"). This seems to be the most comprehensive test of a constitutive equation ever undertaken.

Wagner (18) was able to find a single strain functional h for both shear and uniaxial extension. It is of the form

$$h(t', t) = \exp[-n\sqrt{1 - \alpha} II(t', t) + \alpha I(t', t) - 3] \quad (4)$$

At small strains, the value of h reduces to unity while at large strains $h < 1$.

In most applications, the strain invariants I , II are increasing functions of the time difference $t - t'$. Counterexamples are recovery experiments (e.g., free recovery and extrudate swell). In these cases the minimum value of h

$$h^* = \frac{t''=t}{t''=t'} h(t'', t) \quad (5)$$

should be used in the memory functional (irreversibility assumption of Wagner (18, 19)).

The separation of strain and time dependence in the memory functional has been tested by Laun (16) and by

Osaki (20). In their experiments they observed the relaxation of the first normal stress difference and the shear stress in a step shear strain experiment. The experiments support the factorization in Eq 2.

In the following this constitutive equation will be applied to the analysis of the flow of molten polymers in extrusion dies. In die flow, the material elements are subjected to biaxial extension superimposed on shear flow. The application will actually go beyond the tested region of the constitutive equation: In the rheological experiments, the polymer can only be subjected to unidirectional shear and separately to uniaxial extension. The analysis has been undertaken in spite of these limitations. The reasons are the following:

a) The constitutive equation is applicable to arbitrary strains (shear and extension) when applied in the linear viscoelastic region. Therefore, the achieved results should be reasonably accurate in the limit of slow flow.

b) The large strain behavior of the melt might be described reasonably well by Eq 1. The superposition of shear and extension should be governed by similar strain dependent phenomena as the pure rheometrical experiments in shear or extension. However, there are no rheometers available to test the constitutive equations in this type of flow.

c) The methods developed in this analysis will be available for a more sophisticated analysis, when a more detailed rheological constitutive equation (applicable to complex flows of processing) has emerged.

CALCULATION OF VELOCITY AND STRESS FOR MEMORY INTEGRAL CONSTITUTIVE EQUATIONS

Integral constitutive equations have been used very little in calculating velocity profiles or stress distributions of flowing molten polymers. Marrucci, *et al.* (22) suggested that the integral equation be rewritten as a sum of differential equations (which, of course, is not possible for each type of integral equation) and that these differential equations be solved by established means. The constitutive equation suggested by Marrucci, *et al.* seems to give good agreement between experimental observations and theoretical predictions in shear and uniaxial extension. However, it appears to be more difficult to use than Eq 1.

From the point of view of numerical analysis, differential constitutive equations are appealing because they avoid the complexity of memory integrals. However, in these models the viscoelastic properties of the fluid enter the calculations through terms having high order (like 4th order) derivatives of the velocity. This disadvantage of the approach has led several investigators to develop methods for memory integrals, since they do not demand a high order of differentiability of the velocity field.

Bernstein and Malkus (23) suggest a variational method using a KBKZ constitutive equation (6, 7) with a single time constant. The variational principle is applied to finite elements of fluid. The numerical integration scheme in space and time tracks each spatial integration point from element to element. If, during the course of

tracking of a given particle, the exponential function $\exp(-(t - t')/\lambda)$ becomes sufficiently small, the remaining contribution to the integral may be disregarded, and tracking of that particle terminated. The solution procedure has been applied to flow in the entry region of the contraction of a channel with slit cross-section.

Viriyaayuthakorn and Caswell (24) developed a finite element method where they approximate the memory integral of the constitutive equation by a Laguerre numerical formula. The kinematical problem is the computation of the displacement vector from every node of the numerical grid to the Laguerre points upstream along particle paths. The solution method is restricted to the calculation of non-linear effects as body forces. The method is illustrated with die entry flow in which the fluid is forced through a four-to-one axisymmetric contraction.

Petrie (25) and Wagner (26) used a rheological constitutive equation to predict bubble shapes in the film blowing process. Both used the same rheological constitutive equation with a single time constant. Petrie preferred the differential version (Maxwell model with contravariant time derivative) while Wagner used the integral formulation (rubberlike liquid with one time constant). Wagner additionally incorporated temperature changes during the biaxial extension in the bubble.

The free recovery at the exit of extrusion dies has been calculated by Junk (27) and Wortberg (28), using the superposition principle of linear viscoelasticity. This principle, however, is not applicable to flow in extrusion dies, because the fluid elements are subjected to large strains and the stress-strain relation is non linear. The stress contributions of shear and of extension should not be calculated separately and then added afterwards. The following analysis is quite different from these studies. It will lead to results which are applicable to extrusion at reasonable flow rates.

CALCULATION OF FLOW HISTORY IN ANNULAR EXTRUSION DIES

The annular flow geometry with varying diameter and cross-section is quite common to various extrusion dies. It will be investigated in the following. Note that annular flow includes pipe flow and slit flow as limiting cases.

Integral constitutive equations are most suitable for calculating the stress in a flow of known kinematics. The kinematics in extrusion dies can be calculated by means of very well established numerical solution procedures assuming locally steady shear flow, see Winter (29). The kinematics then will be used to track the fluid elements along their paths in the extrusion die. The deformational (and temperature) history along each path determines the state of the polymer at the exit of the die.

Kinematics of Annular Flow

The simplifying assumptions for calculating the kinematics in annular die flow are the following:

- a) constant temperature throughout the flowing polymer;
- b) no pressure dependence of the rheological properties;

- c) constant density;
- d) lubrication approximation;
- e) shear stress of steady shear flow (locally).

The coordinate system of the following analysis is shown in Fig. 1. Annular flow will be described in cylindrical coordinates (x, r) while the strain history of a fluid element is most easily described in cartesian coordinates (x, y, z) .

The assumption of steady shear flow reduces the x -component of the stress equation of motion into

$$\frac{\partial p}{\partial x} = \frac{1}{r} \frac{\partial}{\partial r} (r\tau_{rx}) \quad (6)$$

where the shear stress τ_{rx} is determined by the local shear rate

$$\dot{\gamma} = \frac{\partial v_x}{\partial r} \quad (7)$$

and the rheological constitutive equation, Eq 1, as applied to steady shear flow:

$$\tau_{rx} = \dot{\gamma} \sum_i \sum_j f_j \frac{\lambda_i G_i}{(1 + n_j \lambda_i |\dot{\gamma}|)^2} \quad (8)$$

The material parameters f_j and n_j describe the large strain behavior. Their values have been determined by Laun (16) for a LDPE melt.

The volume flow rate remains constant with x , since the density is assumed to be constant throughout the flow. The average velocity

$$\bar{v} = \frac{\dot{V}}{\pi(r_a^2 - r_i^2)} = \frac{2}{r_a^2 - r_i^2} \int_{r_i}^{r_a} v_x r dr \quad (9)$$

then adjusts to the change in cross-sectional area along the die.

The velocity profiles are calculated numerically. Typical velocity profiles are shown in Fig. 2.

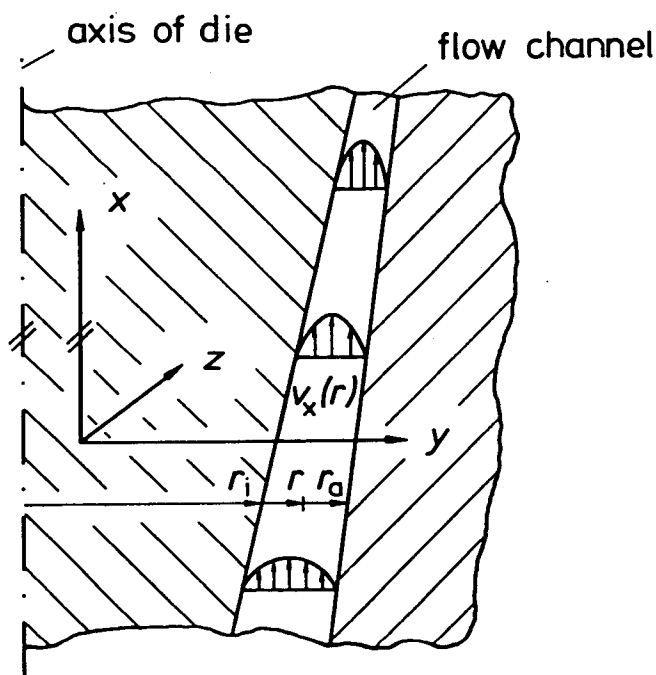


Fig. 1. Coordinate system x, r for annular flow and coordinate system x, y, z for calculating the components of the Finger tensor.

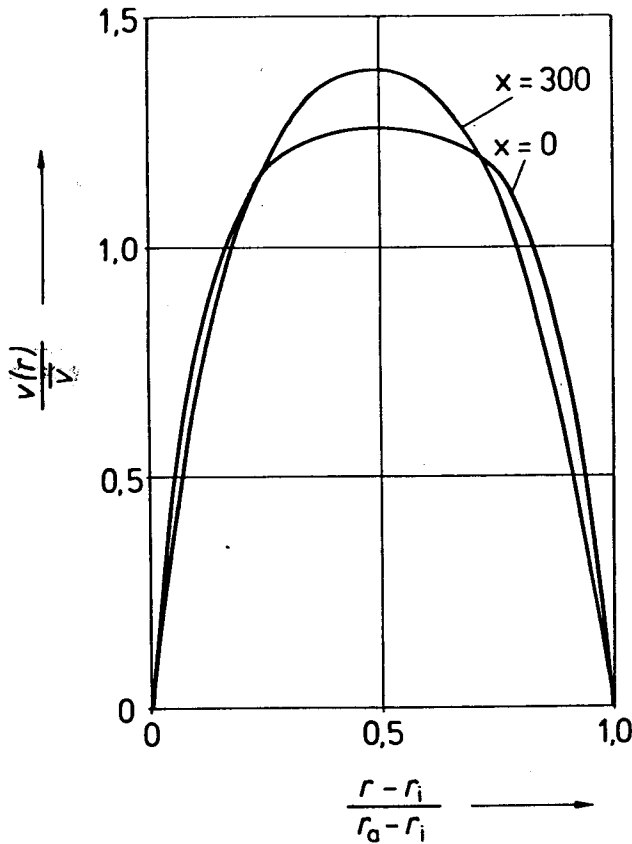


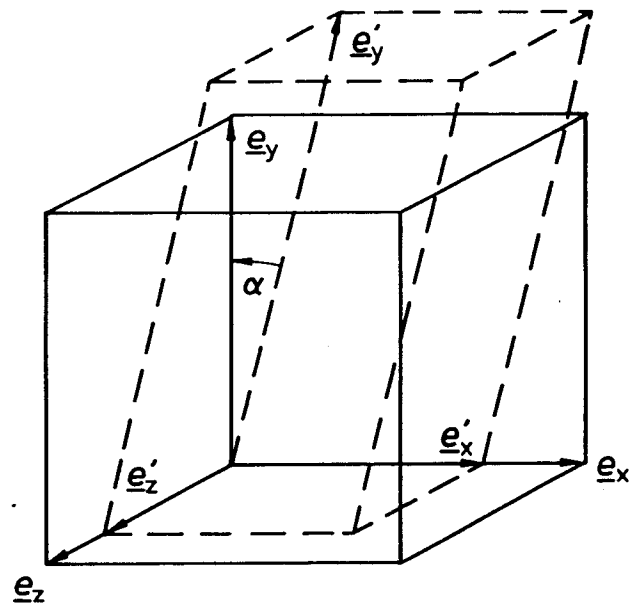
Fig. 2. Velocity distribution at entrance and at exit of annular dies of Fig. 4 (in the Appendix). The flow is assumed to be steady shear flow. Data: $M = 210 \text{ kg/h}$, $T = 180^\circ\text{C}$, rheological properties of LDPE (Laun (17)).

The assumption of locally steady shear flow has been found to be valid when calculating the flow rate as a function of the local pressure gradient $\partial p/\partial x$. Examples are given by Player (30), Wortberg (28), and Junk (27) who approximate an annular flow channel by a sequence of many cylindrical annuli. Brauer (31) and Geiger (32) found that velocity profiles in contained flow develop orders of magnitudes faster than the stress. The kinematics of contained flow seem to be insensitive to the small changes in the stress distribution. The stress of steady shear flow as obtained in a long annulus of constant cross-section can therefore be used to calculate velocity distributions of sufficient accuracy, even if the cross-section of the annulus changes in the flow direction.

The kinematics will be used for calculating the deformation of a fluid element along its path and for calculating the corresponding stress tensor.

Components of the Relative Deformation Tensor

A fluid element is sheared and stretched when flowing through an extrusion die, see Fig. 3. The volume is assumed to stay constant. The deformation is described by three material vectors \underline{e}_i which form an orthonormal system at time t . At previous times $t' < t$, the material vectors form a nonorthonormal coordinate system \underline{e}'_i whose metric is the Cauchy-Green tensor \underline{C} . Its inverse will be used to calculate the stress at time t , see Eq 1. The orthonormal system \underline{e}_i is chosen to be the system x, y, z of Fig. 1.



$x = \text{flow direction}$
 $y = \text{radial direction}$
 $z = \text{circumferential direction}$
 shear $\gamma = \tan \alpha$

Fig. 3. Deformation $t' \rightarrow t$ of a material element. Definition of the material vectors $\underline{e}_i = \underline{e}_i(t)$ and $\underline{e}'_i = \underline{e}_i(t')$ and of the relative shear strain γ .

The components of the Finger tensor are

$$(\underline{C}^{-1}) = \begin{pmatrix} (1 + \gamma^2)/\delta_x^2 - \gamma\delta_z & 0 \\ -\gamma\delta_z & 1/\delta_y^2 & 0 \\ 0 & 0 & 1/\delta_z^2 \end{pmatrix} \quad (10)$$

where

$$\delta_x = e'_x/e_x \quad (11)$$

$$\delta_y = e'_y \cos\gamma/e_y \quad (12)$$

$$\delta_z = e'_z/e_z \quad (13)$$

are the dilatations in the three directions with

$$\delta_x \delta_y \delta_z = 1 \quad (14)$$

at constant density. The shear angle γ is just the integral of the shear rates along a stream line ($\psi = \text{const}$) from t to t'

$$\gamma(t') = \int_t^{t'} \dot{\gamma}(t'') dt'' ; \gamma(t) = 0 \quad (15)$$

Note that Eq 10 does not describe the most general kind of deformation at constant volume, where the superposition of shear and extension would be arbitrarily. In Eq 10 the shear and the extension are chosen such that the shear direction and the normal to the shear plane are principal directions of the extensional flow component. The shear plane ($x - z$ - plane) changes its area due to the extensional component.

Tracking of a Fluid Element

The radial position of a fluid element is prescribed by its value ψ of the stream function, which stays constant along the paths in the annulus. The stream function

$$\psi(r) = \frac{\int_{r_i}^r v_r(r) r dr}{\int_{r_i}^{r_a} v_r(r) r dr} = \frac{2}{(r_a^2 - r_i^2)\bar{v}} \int_{r_i}^r v_r(r) r dr \quad (16)$$

is equal to zero at the inner wall and equal to 1 at the outer wall of the annulus.

The axial position x of a fluid element corresponds to time t while position x' corresponds to t'

$$t(\psi) - t'(\psi) = \int_{x'}^x \frac{dx}{v_x(\psi)} \quad (17)$$

The integration has to be carried out at constant ψ .

The shear strain $\gamma(t', \psi)$ is evaluated by integrating Eq 15 along the stream line.

The stretch in flow direction is given by the change of velocity along a stream line:

$$\delta_r(t', t, \psi) = \frac{e_r'}{e_r} = \frac{v_x(t', \psi)}{v_x(t, \psi)} \quad (18)$$

The stretch in circumferential direction corresponds to a change of radial position of the stream line

$$\delta_z(t', t, \psi) = \frac{e_z'}{e_z} = \frac{r(t', \psi)}{r(t, \psi)} \quad (19)$$

These strain variables will be calculated from the kinematics of the flow in the extrusion die. They will be put into the Finger tensor (Eq 10) and the strain functional h , Eq 4.

RESULTS OF THE CALCULATION

In the calculations, the temperature will be assumed to be constant. The rheological constitutive equation will be applied to study flow which is a superposition of shear and biaxial extension. The material parameters in the constitutive equation are the ones of low density PE ("Melt I") as measured by Laun (16).

The annular flow geometry with varying diameter and cross-section has been applied to the three die geometries of Fig. 4 and to an annulus of constant cross section. These three geometries are chosen to demonstrate the magnitude of the phenomena. The analysis, of course, is also applicable to other annuli. The mass flow rate $\dot{M} =$

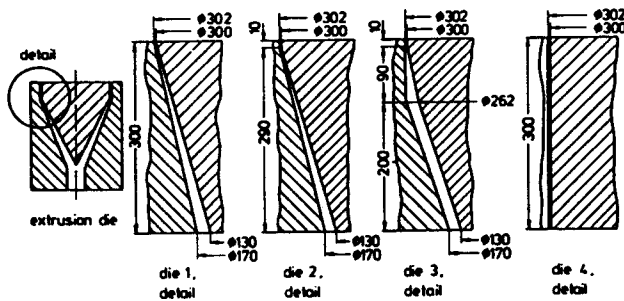


Fig. 4. Sketch of three annular die geometries to be investigated. The inlet geometry (130 mm to 170 mm), the exit geometry (300 mm to 302 mm), and the length are the same for all three dies. For comparison, a fourth geometry will be used: An annulus of cross section (300 mm to 302 mm) which is constant throughout. It will be called "die 4".

210 kg/h and the temperature $T = 180^\circ\text{C}$ is chosen to be the same in all the following examples.

Stress Ratio $N_1/2\tau_{12}$ at Die Exit

The stress at the exit of the extrusion die is a measure of the memorized flow history of processing in the die. We therefore calculate the normal stress difference distribution $N_1(\psi) = \sigma_{xx} - \sigma_{yy}$ and the shear stress distribution $\tau_{12}(\psi) = \tau_{xy}$ from the kinematics as calculated above. In steady shear flow at small shear rates, the ratio of these stresses has been predicted to be equal to the recoverable shear strain (33)

$$\gamma_r = \lim_{t' \rightarrow -\infty} \frac{N_1}{2\tau_{12}} \quad (20)$$

Laun (34) has found experimentally that this relation also holds for steady shear flow outside the linear viscoelastic region.

Flow in extrusion dies cannot be considered to be steady shear flow, even if the kinematics are locally very similar to the kinematics of steady shear flow. In Fig. 5 the stress ratio as calculated for the three extrusion dies is compared with the corresponding stress ratio at the exit of "die 4" which is an annulus of constant cross-

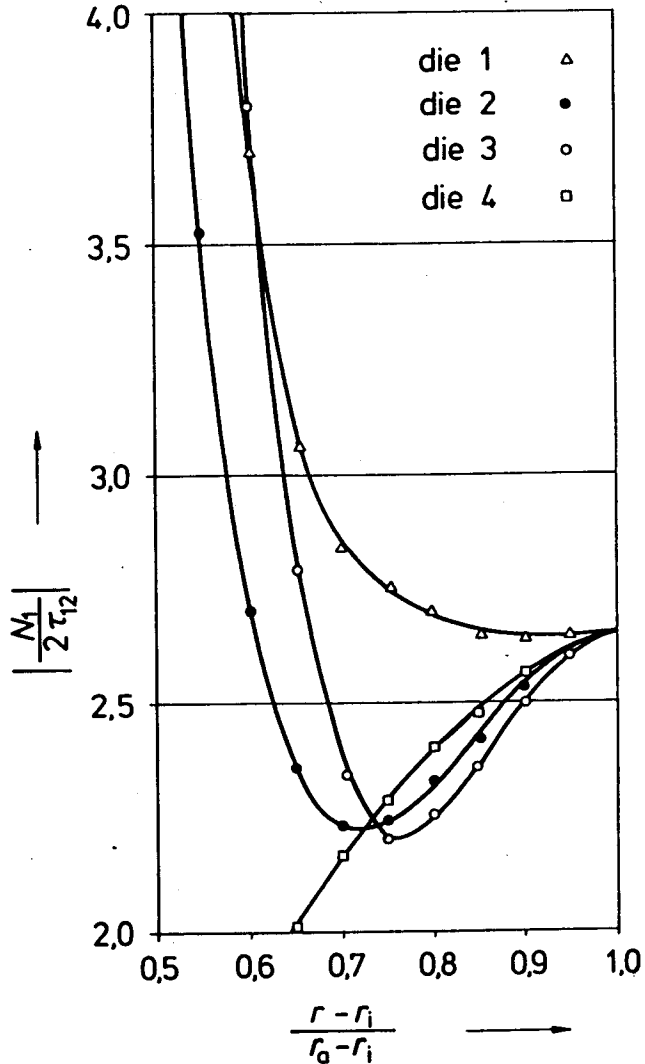


Fig. 5. Stress ratio at exit of extrusion dies of Fig. 4. The points are calculated numerically using rheological data of Laun (16) with $\dot{M} = 210 \text{ kg/h}$, $T = 180^\circ\text{C}$.

section throughout. The difference is very pronounced: The largest stress ratios are found in "die 1" and "die 2." The stress ratio in "die 2" is much smaller already than in the annulus of constant cross section ("die 4"). Tapered sections seem to increase the stress ratio significantly (due to the extensional flow component), while shear flow reduces the stress ratio to a smaller value.

Close to the wall, the stress ratios approach the same value for all four dies, since the flow approaches steady shear flow at the wall (a result which is true for any steady contained flow, when the non-slip condition applies (35). There is, however, only a small fraction of the extruded polymer which originates from a layer near the walls. The largest fraction of the polymer passes through the middle of the annulus, where the differences between the four dies are most pronounced. Figure 5 shows how small changes in die geometry affect the state of the extruded polymer.

The stress ratios of Fig. 5 have been calculated by numerical integration of Eq 1 using Eqs 2, 3, and 10 and the numerically determined velocity distribution in the entire flow channel of the dies.

Due to the fading memory of the polymer as described in Eq 2, the integration does not have to be performed in the complete range $[-\infty < t' < t]$. There is only a finite time t' in the past and a corresponding position x^* in the die, beyond which the upstream strain history of a fluid element has no influence any more. The memory to previous deformations has faded due to large residence times or due to large new strains closer to the die exit. When designing an extrusion die, one should know the extent of influential strain history in the die. The extrusion die then can be designed to impose the desired strain history onto the flowing polymer.

It should be mentioned here that the present calculations are not applicable to flows with a memory which reaches upstream into spider sections or streaker plates. The calculations, however, can tell whether the strains in the annular flow channel are sufficiently large to erase the memory of such undesired upstream flow histories.

Figures 6 and 7 show values of the stress ratio as obtained from integrations from $t' = t'(x^*)$ in the die to $t' = 0$ at the die exit. The value x^* describes an upstream distance from the die exit. With increasing x^* the memory integral adopts a constant value at $x^* = l_m$ and the integration can be terminated. The magnitude of l_m depends on the strain history along the stream lines (and the rheological properties of the polymer, of course). Close to the middle of gap, the fluid elements move the fastest while subjected to the smallest strains (extension only); in that region, the memorized flow history may reach very far upstream and may give rise to undesired properties of the extrudate. In Fig. 6, a stream line near the middle has been investigated to show the positive influence of tapered sections. The length l_m of the influential strain history is much shorter in the first three dies than in "die 4" of constant cross-section.

Free Recovery at the Die Exit

A possible experimental measure of recoverable strain is extrudate swell, i.e., the increase in cross-sectional area of the polymer stream when leaving the

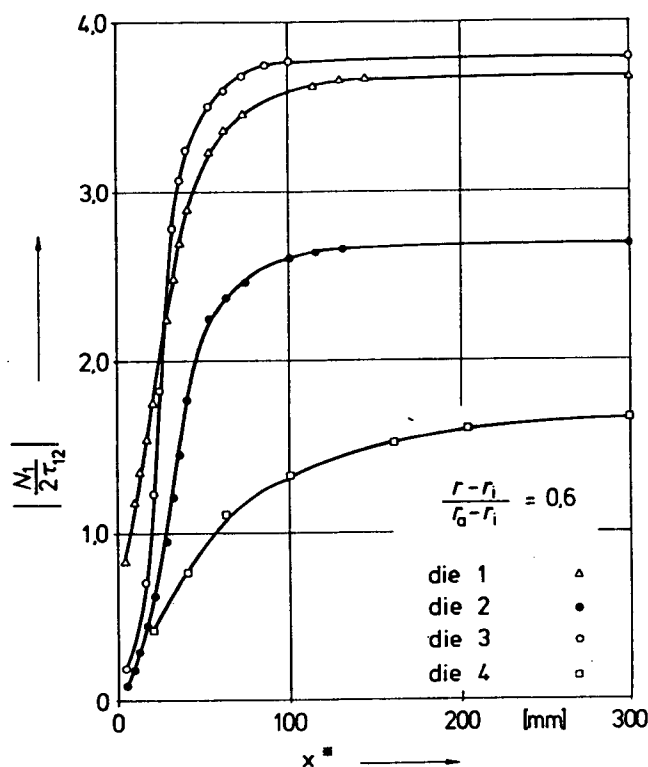


Fig. 6. Stress ratio (calculated points) as determined by numerical integration from $x = 0$ to $x = x^*$. Fluid element near the middle of the annulus. For data see Figs. 4 and 5.

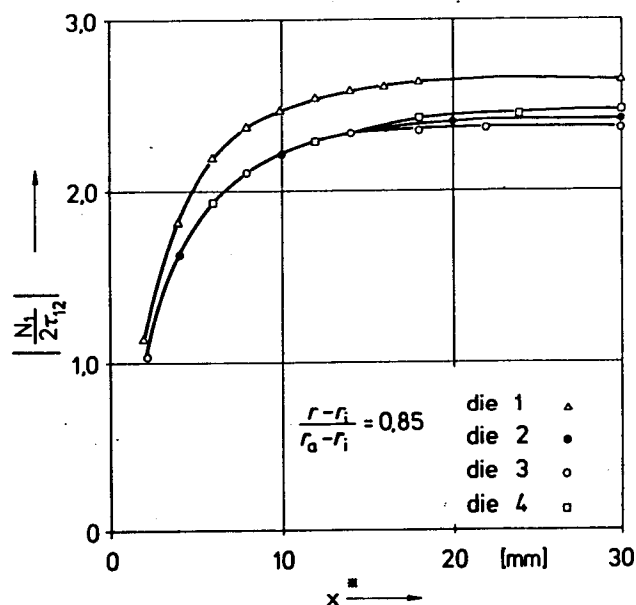


Fig. 7. Axial development of stress ratio (calculated points). Fluid element near the wall of the annulus.

extrusion die. This area-change is observed with time and related to the strain history in the die. Extrudate swell, however, is an integral measure which smoothes out inhomogeneities within each cross section. It cannot distinguish between the recoverable strain of an element near the surface of the extrudate and an element in the middle. In the following we therefore propose a hypothetical experiment which gives detailed insight in the effects of the inhomogeneous strain history across the extrusion die.

It is assumed that the extrudate at the die exit is instantaneously chopped into small elements of homogeneous strain history. The isothermal free recovery of these elements is observed in a computer "experiment." The distribution of free recovery across the annular gap will give a detailed insight on the flow process in extrusion dies. Changes in die geometry or differences in the rheological properties can be analyzed in detail.

Each polymer element in the extrusion die undergoes shear and biaxial extension. At time $t = 0$ the stress is made isotropic. We require the instantaneous and the delayed recovery at times $t \geq 0$. The equation of the stress becomes

$$\underline{\sigma}(t) = \underline{0} = -p\underline{1} + \int_{-\infty}^0 [m\underline{C}^{-1}]_d dt' + \int_0^t [m\underline{C}^{-1}]_r dt' \quad (21)$$

where $[m\underline{C}^{-1}]_d$ = memorized strain history of polymer element along the stream line in the extrusion die and $[m\underline{C}^{-1}]_r$ = memorized strain history during free recovery at constant temperature. The strain is described with an orthonormal base in state $t' = t$. This is different from the analysis of Lodge, *et al.* (33, 36) who used an orthonormal base in the state at $t = 0$ (corresponding to the die exit) and determined the equivalent rubbery response.

The equation of the stress can be broken up into components

$$0 = \left[\int_{-\infty}^0 + \int_0^t \right] m(C_{xx}^{-1} - C_{yy}^{-1}) dt' \quad (22a)$$

$$0 = \left[\int_{-\infty}^0 + \int_0^t \right] m(C_{yy}^{-1} - C_{zz}^{-1}) dt' \quad (22b)$$

$$0 = \left[\int_{-\infty}^0 + \int_0^t \right] m C_{xy}^{-1} dt' \quad (22c)$$

and solved together with Eq 10 for $\delta_r(0, t, \psi)$, $\delta_y(0, t, \psi)$, $\delta_z(0, t, \psi)$, and $\gamma_r = \gamma(0, t, \psi)$. The recovery is a function of time ($t > 0$) and of the stream function ψ .

The system of equations has been solved numerically. For $t = 0^+$, there is a small spontaneous recovery, due to the discrete choice of relaxation spectrum. This spontaneous recovery, however, was found easy to calculate by using a linearly changing strain (ramp) between $t' = 0$ and $t' = 10^{-5}$ s. $t' = 0$ corresponds to the beginning of the free recovery "experiment."

The value of t is increased stepwise until the complete recovery is achieved after about 100 s. Results of the calculations are shown in Fig. 8. The annulus of constant cross section ("die 4") exhibits the smallest recovery. It is the same in both directions; this is a result which agrees with a similar calculation by Lodge (33). For the other dies, the relative increase in thickness δ_y^{-1} is larger than the swelling in circumferential direction δ_z^{-1} , which would correspond to a diameter increase of the extrudate.

The distribution of recovery across the exit of the dies is shown in Fig. 9. Close to the wall, the recovery approaches the value corresponding to steady shear flow. The largest differences are found in the middle of the annulus. Note that at $(r-r_i)/(r_o-r_i) = 0.5$ the fluid elements can pass "die 4" without being deformed; the

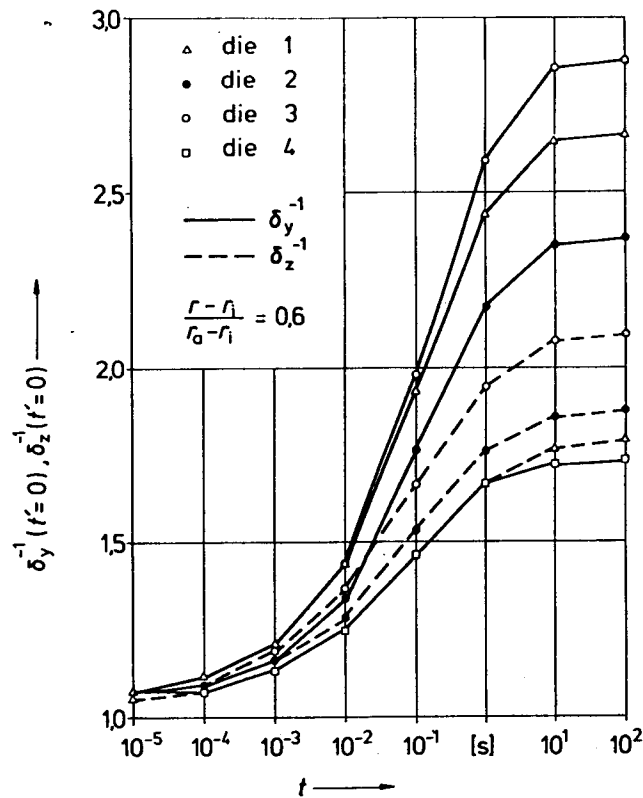


Fig. 8. Recovery of fluid elements at the exit of the annular dies of Fig. 4 as compared to the recoil at the exit of an annulus of constant cross section throughout ("die 4"). The points are calculated using rheological data of Laun (16).

corresponding recovery values are unity (no "recovery").

Corresponding recovery angles γ_r are given in Fig. 10 and Fig. 11. The differences between the dies are less pronounced with respect to γ than in the dilational measurements.

CONCLUSIONS

The state of the polymer at the exit of an extrusion die depends on the properties of the polymer and on the processing history. Small differences in die geometry result in large differences of the stress ratio $N_1/2t_{12}$ and the possible free recovery at the die exit. The memory of the polymer on the upstream processing history is erased by large strains in the flow. The new strain history near the die exit determines the state of the extrudate.

The influence of die geometry is demonstrated on three diverging annular dies and one annulus of constant cross section. In an annulus of constant cross section, the polymer elements are subjected to shear only. The magnitude of the shear strain depends on the radial position: for a path near the wall, the shear strain is very large, while the fluid element in the middle of the annulus flows along without being deformed at all. In a diverging or converging annulus, the polymer elements are additionally subjected to biaxial extension. This additional deformation does not only affect the polymer elements which move close to the wall, but also the ones in the middle of the annulus. Opening and narrowing of the die channel are important features of die design,

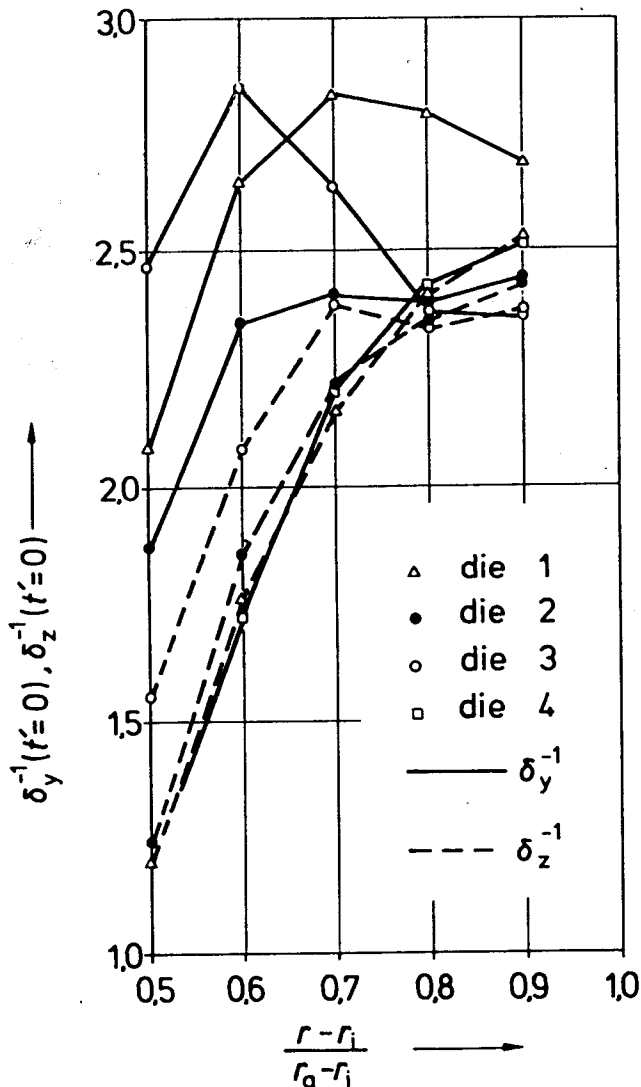


Fig. 9. Recovery of fluid elements after 100s. The points are calculated.

because they make it possible to erase the memory on upstream processing history, even if the material element flows in the middle of the channel.

The three dies of varying cross section are purposely chosen to be very similar to each other: same entrance cross section, same exit cross section, same length. As a consequence, the same distribution of extensional strains has been imposed on the polymer elements across the three annuli. The only differences are the time scale of the extension and the magnitude of the shear strains. Still, the differences in the state at the die exits are very large. In actual die design, the choice of die geometries would be less restricted and would result in an even larger spectrum of achievable states. The proposed method of analysis will be a tool to choose the appropriate die geometry.

ACKNOWLEDGMENT

The research has been supported by the Deutsche Forschungsgemeinschaft. The major part of the study has been undertaken while HHW was at the University of Stuttgart. We are grateful to Mr. R. Wolff for his help in the numerical computations.

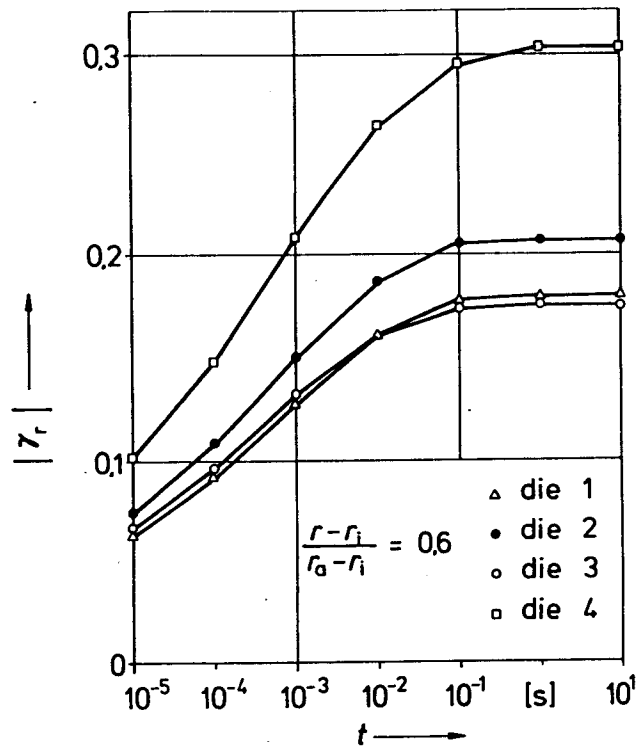


Fig. 10. Changing shear angle of extrudate elements during free recovery. Notation: $\gamma_r = \gamma(t' = 0, t, \psi)$.

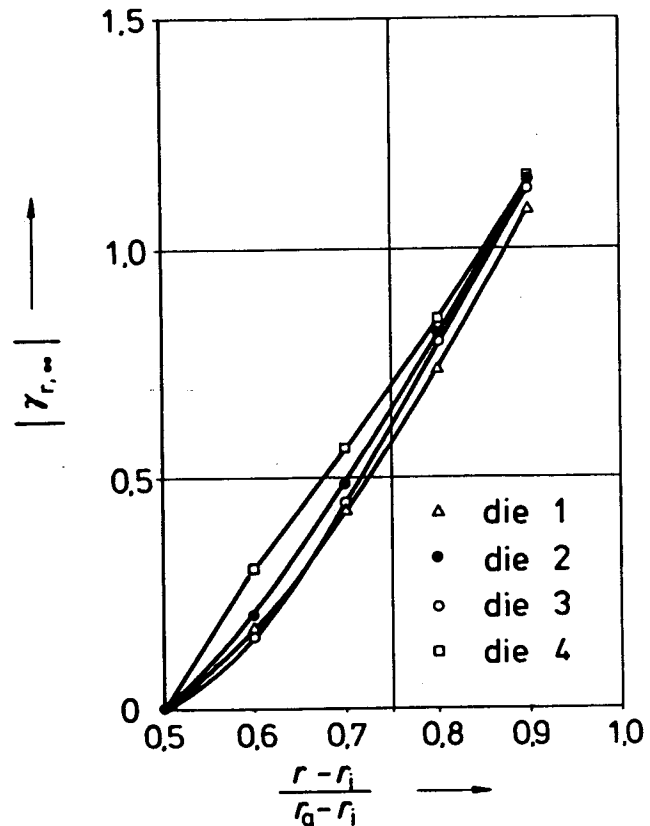


Fig. 11. Calculated recovery angles of the material elements after 100s.

NOMENCLATURE

- $\underline{C}^{-1}(t', t)$ = relative Finger strain tensor, -
- d = diameter of annulus, m
- e_i = embedded vectors

- f_i = rheological material parameter, see Eq 8, Ref. (16)
- G_i = relaxation moduli of linear viscoelasticity, Pa
- h = strain functional, -, see Eq 2
- l = length of die, m
- $m(t', t)$ = memory functional, Pa s^{-1} , see Eq. 2
- $\dot{m}(t-t')$ = memory function of linear viscoelasticity, Pa s^{-1}
- \dot{M} = mass flow rate, kg/h
- n = rheological parameter of strain functional h , -, see Eq 4
- N = number of relaxation times of discrete relaxation spectrum, -
- N_1 = first normal stress difference, Pa, $\tau_{xx} - \tau_{yy}$
- p = pressure, Pa
- r = coordinate, m
- t = time, s
- v = velocity, m/s
- \dot{V} = volume flow rate, m^3/s
- x, y, z = coordinates, m
- α = rheological material parameter, -, see Eq 4
- γ = shear strain, -
- $\dot{\gamma}$ = shear rate, s^{-1} , see Eq 7
- δ_r = stretch in flow direction, -
- δ_y = stretch in radial direction, -
- δ_z = stretch in circumferential direction, -
- λ_i = relaxation time of linear viscoelasticity, s
- ω = angular frequency, s^{-1}
- ψ = stream function, -, see Eq 16
- σ = stress, Pa
- $\bar{\tau}$ = extra stress, Pa
- I, II, III = invariants of Finger strain tensor

Indices

- a = at outer wall
- d = inside die
- i = at inner wall
- r = recovery outside die

REFERENCES

1. Z. Tadmor and C. G. Gogos, "Principles of Polymer Processing," Wiley, New York (1979).
2. J. L. Throne, "Plastics Process Engineering," M. Dekker, New York, (1979).
3. S. Middleman, "Fundamentals of Polymer Processing," McGraw-Hill, New York, (1977).

4. R. B. Bird, R. C. Armstrong, and O. Hassager, "Dynamics of Polymeric Liquids," Wiley, New York (1977).
5. A. S. Lodge, *Trans. Faraday Soc.*, **52**, 120 (1956).
6. A. Kaye, College of Aeronautics, Note 134, Cranfield (1962).
7. B. Bernstein, E. A. Kearsley, and L. J. Zapas, *Trans. Soc. Rheol.*, **7**, 391 (1963).
8. J. O. Doughty and D. C. Bogue, *Ind. Eng. Chem. Fundam.*, **6**, 388 (1967).
9. R. I. Tanner and G. Williams, *Trans. Soc. Rheol.*, **14**, 19 (1970).
10. H. C. Yen and L. V. McIntire, *Trans. Soc. Rheol.*, **18**, 495 (1974).
11. M. H. Wagner, *Rheol. Acta*, **15**, 136 (1976).
12. M. C. Phillips, *Trans. Soc. Rheol.*, **20**, 185 (1976).
13. K. Osaki, S. Otha, M. Fukuda, and M. Kurata, *J. Polym. Sci.*, **14**, 1701 (1976).
14. M. Doi and S. F. Edwards, *Faraday Trans. II*, **74**, 1789 (1978); **74**, 1802 (1978); **74**, 1818 (1978); **75**, 38 (1979).
15. M. H. Wagner, *Rheol. Acta.*, **15**, 136 (1976).
16. H. M. Laun, *Rheol. Acta.*, **17**, 1 (1978).
17. M. H. Wagner and H. M. Laun, *Rheol. Acta.*, **17**, 138 (1978).
18. M. H. Wagner, *J. Non-Newtonian Fluid Mech.*, **4**, 39 (1978).
19. M. H. Wagner and S. E. Stephenson, *J. Rheology*, **23**, 489 (1979).
20. K. Osaki, N. Bessho, T. Kojimoto, and M. Kurata, *J. Rheology*, **23**, 457 (1979).
21. J. D. Ferry, "Viscoelastic Properties of Polymers," John Wiley, New York (1970).
22. G. Marrucci, G. Titomanlio, and G. C. Sarti, *Rheol. Acta*, **12**, 269 (1973).
23. B. Bernstein and D. S. Malkus "A variational principle of visco-elastic memory fluids and its use in finite element analysis of steady flows," Preprint, Dept. of Mathematics, Illinois Institute of Technology, Chicago, Ill. 60616.
24. M. Viriyayuthakorn and B. Caswell, *J. Non-Newt. Fluid Mech.*, **7**, 245 (1980).
25. C. J. S. Petrie, *AIChE J.*, **21**, 275 (1975).
26. M. H. Wagner, Dissertation, University Stuttgart (1976).
27. P. B. Junk, Dissertation TH Aachen (1978).
28. J. Wortberg, Dissertation TH Aachen (1978).
29. H. H. Winter, *Adv. Heat Transfer*, **13**, 205 (1977).
30. O. Player, *Plastverarbeiter*, **20**, 693 (1969).
31. H. Brauer, "Grundlagen der Ein- und Mehrphasenströmung," Sauerlander, Aarau (1971).
32. K. Geiger and H. H. Winter, "Rheologische Einlaufstrecke für die Spalt-Strömung einer elastischen Flüssigkeit," Jahrestagung Deutsche Rheol. Gesellschaft, Aachen (1979).
33. A. S. Lodge, "Elastic Liquids," Academic Press, London, New York (1964).
34. H. M. Laun, "Elastische Deformationsanteile bei der Dehnung und Scherung von Kunststoffschmelzen", Jahrestagung Deutsche Rheol. Gesellschaft, Aachen (1979).
35. H. H. Winter, *Polym. Eng. Sci.*, **15**, 460 (1975).
36. A. S. Lodge, D. J. Evans, and D. B. Scully, *Rheol. Acta*, **4**, 140 (1965).